NIRSPEC

UCLA Astrophysics Program **U.C. Berkeley** **W.M. Keck Observatory**

Don Figer

May 7, 1996

NIRSPEC Optics Design Note 7.01
Front-end and Keck II Telescope (f/15)

I. Introduction

This document describes the system design parameters and lens designs for the NIRSPEC front-end optics, including all elements from the window to the slit. The system design parameters were essentially fixed in the NIRSPEC proposal document with the notable change that the instrument will now be at the f/15 focus of the telescope; these parameters will be summarized and embellished here.

The preliminary lens designs were investigated throughout the period from the proposal phase to past the Preliminary Design Review (PDR). The final designs are presented here with a brief mention of a refractive alternate design for the f/converter. Preliminary design forms were discussed in previous versions of this design note, i.e. NODN 7.00.

II. NIRSPEC System Design Requirements

The system requirements have been prescribed in the following internal documents: the NIRSPEC proposal (4/6/94), the Specification Summary presented at the NIRSPEC project meeting #3 (12/7/94), NODN 1.00, the Preliminary Design Review document (6/1/95), and the Critical Design Review document (2/8/96). In some cases, the requirements in earlier documents were modified somewhat and redefined in the later documents. The requirements are repeated below where the primary optical track contains optics which pass light from the target to the spectrometer. The support optics ensure that the object is kept within the slit during the exposure and that the data can be calibrated.

A. Primary Track

- f/15 input beam from telescope
- the telescope focal plane will be just outside the instrument window
- image derotation (> 360°)
- position angle selection for slit on the sky (360°)
- collimate the f/15 input beam and form a pupil image, d < 30 mm
- provide a pupil mask (Lyot stop) at the pupil image
- > 10 selectable order-sorting filters
- focus the collimated beam at f/10 onto the slit-plane
- 80% ensquared energy into one spectrometer pixel at the slit-plane
- achromatic between 1-5 μm
- maintain all requirements after repeated thermal cycling
- 300 circular field of view (FOV) for the spectrometer
- baffling to ensure < 0.1 photons/s/pixel at the spectrometer detector
- selectable slit sizes: widths from 002 to 106 in steps of 002 and lengths up to 300
- package size consistent with total dimensions of 2.0 m X 0.75 m X 0.75 m for the whole instrument

B. Support Modules

- an external, optical guider camera
  - + plate scale for critically sampling the seeing disk
  - + FOV to ensure a high probability of finding a guide star
  - + minimal moving parts and cost
- an internal, infrared slit-viewing camera (SCAM)
  - + 460 × 460 FOV
  - + 256x256 HgCdTe array
- an external, automatically moveable, calibration unit to provide
  - + flat-field
  - + wavelength calibration
  - + a map of the slit location
  - + an f/15 output beam

III. The Keck II Telescope at f/15

The properties of the Keck II telescope with the f/15 secondary are summarized in Table 1. Most of these parameters were taken from a fax dated 10/8/93 sent by James Graham; these numbers are the same as those in the Keck Observatory Technical Note 163. A few additional parameters were derived. The inscribed diameter of the primary was derived by geometric construction. The exit pupil-focal plane distance is derived below.

The Keck II primary is the entrance aperture for the telescope and it is coincident with the entrance pupil. It has a focal length equal to 34.974/2 = 17.487 m. An image at prime focus cannot be formed because the secondary is 2.092015 m closer to the primary than this distance; however, this virtual image can be used as the object for the secondary. The secondary, then, forms an image at $(1/2.092015 - 1/2.368958)^{-1} = 17.895$ m away from the secondary, giving a back focal length of 17.895 − 15.394985 = 2.5 m.

The secondary also forms a virtual image of the primary, defining the exit pupil of the telescope. This virtual image is at $(1/2.368958 + 1/15.394985)^{-1} = 2.0530393$ m behind the secondary. So, to NIRSPEC, the pupil appears to be 19.948024 m beyond the telescope focal plane.

The Keck telescope is diffraction limited at NIR wavelengths where the optical path difference (OPD) for field points within a radius of 30″ is $< \lambda_{1.00\ \mu m}/60$ peak-to-valley assuming a curved image plane with a radius of 2.123573 m as shown in Table 1. The performance degrades negligibly for a flat image plane, where this OPD is $< \lambda_{1.00\ \mu m}/14$.

Table 1: Optical properties of the Keck II telescope with f/15 secondary

parameter	value	units
Primary:		
radius of curvature	34.9740	m
diameter (inscribed)	9	m
diameter (circumscribed)	10.949	m
conic constant	! 1.003683	
Secondary:		
radius of curvature	! 4.737916	m
diameter (0° FOV)	1.309857	m
diameter (inc FOV)	1.399421	m
conic constant	! 1.644326	
Effective focal properties:		
back focal distance	2.500	m
final focal length	149.583	m
primary-secondary distance	15.394985	m
exit pupil-focal plane distance	19.948024	m
focal radius of curvature	2.123573	m
field size for 20N FOV	0.870	m
f/15 FOV radius	10.00	N
Aberrations:		
coma at 10N radius	! 0.005	O
astigmatism at 10N radius	0.506	O

IV. Optical System Design Requirements for Front-end

The front-end optical design has been divided into 2 sections or modules, the Image Rotator (IROT) and the f/converter imager (FCON). In addition, there are 3 modules which provide support functions for the spectrometer: the Calibration Unit, the Guider Camera, and the Slit-Viewing Camera (SCAM). The first two of these modules are not affected by the optical properties of optics

within the dewar, but the SCAM receives light after having gone through the front-end optics up to the slit. The Guider Camera optics do not affect the beam going into the dewar because it images an annular field surrounding the SCAM FOV. The Calibration Unit optics do not pass light from sky field points, although it is supposed to simulate these field points. These optical relationships are represented in Figure 1. The figure only gives a crude representation of the relative positions of optical modules along the optical train.

In the final design, the IROT actually provides three functions: image derotation, collimation, and pupil image formation. The FCON accepts the collimated beam from the IROT and forms an image of the field at the slit-plane. The optical properties of the beam are summarized in Table 2, where the FOV is circular with d = 32.50; the pupil diameter is taken to be 10 m. These numbers were derived by assuming the required FOV, parameters of the Keck II f/15 telescope, and the output f/number. The actual properties of the beam in a real design will deviate, by some small amount, from these numbers. For instance, the output beam will not be perfectly telecentric.

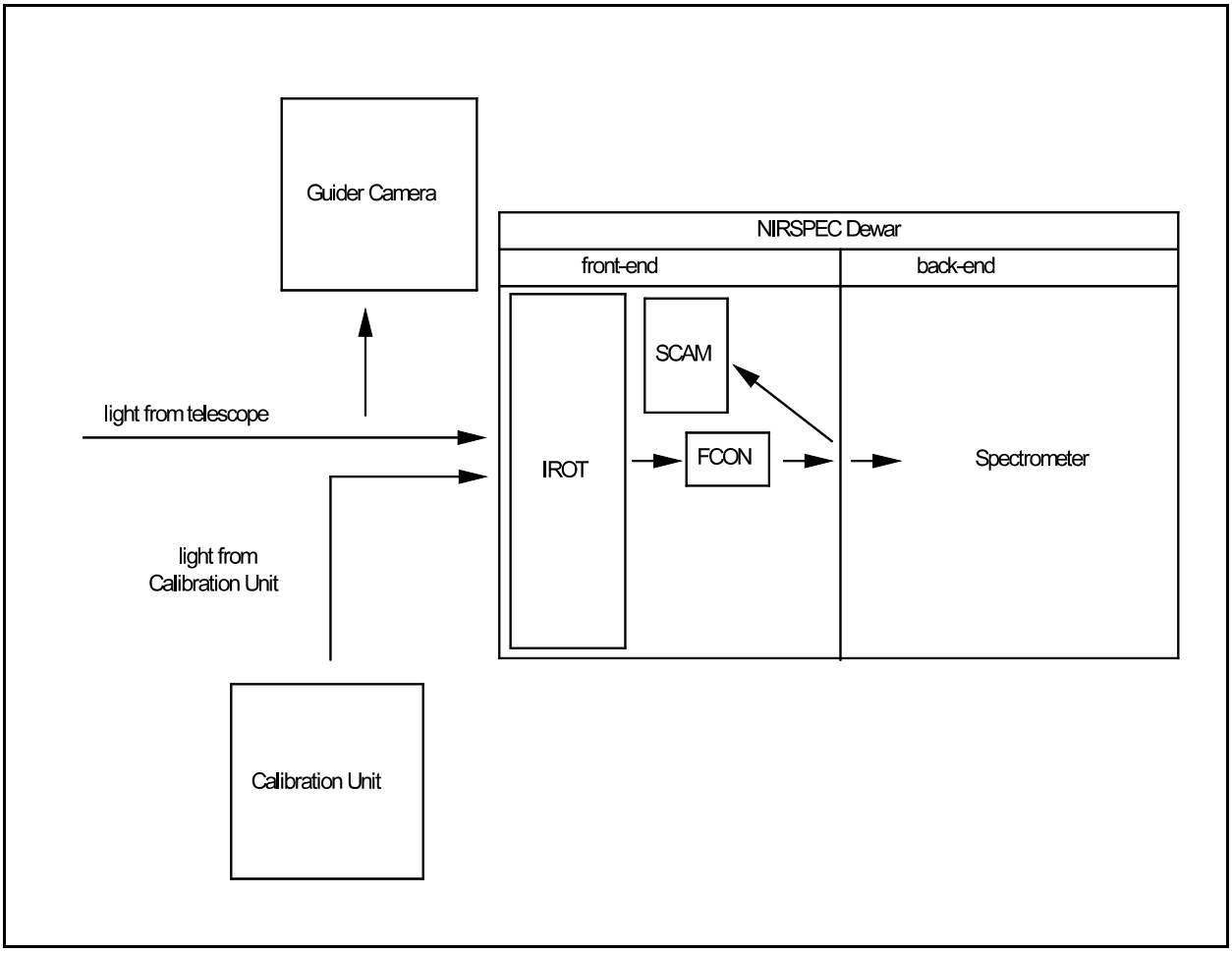

Figure 1. Block diagram of NIRSPEC optics showing detail in the front-end.

Table 2: Properties of beam

Location	Output Angle Between Extreme Chief Rays	Output Angle Between Marginal Rays for Axial Field Point	Output Beam	
primary	650 = 0°0181	32°5	converging	f/1.75
secondary	0°1375	3°8	converging	f/15
focal plane	0°1375	3°8	diverging	f/15
window	0°1375	3°8	diverging	f/15
collimator	16°94	0°	collimated	-
Lyot stop	6°92	0°	collimated	-
f/converter	0°	5°72	converging	f/10
slit	0°	5°72	diverging	f/10

V. First-order Properties of the Front-end

Knowing the system requirements, we can calculate the required focal lengths and distances of the various optical elements in the front-end. We can assume ideal lenses for this purpose.

The internal pupil image size should be less than 30 mm according to the requirements listed at the beginning of this document; there is no other constraint giving the exact size of this image. The collimating mirror can be placed at an apparent distance beyond the telescope focal plane equal to its focal length; this will ensure that the lens forms a collimated beam. In this context, "apparent" means that the telescope focal plane appears as if it is that far from the collimator. This distinction must be made because the beam will pass through a window before reaching the collimator, and the window will produce an apparent longitudinal shift in the location of the telescope focal plane. In any event, the total apparent distance between the telescope focal plane and the collimating lens was chosen to be 400 mm. This choice is somewhat arbitrary and really only sets the size of the pupil image to be $F_{coll}/f\#_{tele}$ = 400 mm/14.9583 = 26.741 mm. The f# for the telescope was calculated as F_{tele}/10 m, where F_{tele} = 149.583 m as shown in Table 1.

The location of the pupil image can be calculated using the thin lens formula shown in equation 1. The apparent distance between the telescope focal plane and the collimator is 400 mm. The distance from the telescope exit pupil to the telescope focal plane is 19.948024 m, as given in Table 1. So, the distance between the collimator and the pupil image is 408.021 mm.

$$d_{collimator-pupil\ image} = -\left(\frac{1}{d_{apparent,fp-collimator} + d_{exit\ pupil-fp}} - \frac{1}{F_{apparent}} \right)^{-1} \quad \textbf{(1)}$$

The f/converter should refocus the beams at f/10, as stated earlier. The pupil size for this lens is 26.741 mm, so the apparent focal length of the lens should be 267.41 mm. Also, the output beams from the f/converter should be nearly telecentric so as to present an exit pupil at infinity to the back-end optics (this is discussed further below). Again, using the thin lens formula, we find that the pupil image will be transferred to infinity if the distance between it and the lens is equal to the focal length of the lens. This means that the distance between the Lyot stop and the f/converter will be equal to the distance between the f/converter and the slit plane.

Table 3 contains the numbers derived above or shown in Table 1. These numbers were calculated assuming 6 significant digits to the right of the decimal.

Table 3: Properties of ideal optics
all units are meters

Element	Apparent Distance to Next Element	Apparent Focal Length	Beam Size[1] or Field Size [2]
primary	15.394985	17.487000[a]	10.000000
secondary	17.894980[a]	2.368958	-
image of primary	-	-	1.333577
telescope f.p.	0.400000	-	0.033359
IROT/collimator	0.408021	0.400000	-
filter/Lyot stop	0.267410	-	0.026741
f/converter	0.267410	0.267410	-
slit f.p.	-	-	0.022239

[1]for axial field point - only listed where pupil image is formed
[2]size of one side of square field (460 X 460) - only listed where image is formed
[a]zeros padded on the right

VI. Image Rotator Design

The image rotator performs three functions: image derotation, collimation, and pupil image formation. There were not any quantitative goals concerning these functions listed in the specification documents; however, some of these were derived by considering other performance goals.

For instance, the centroid of an emission-line on the detector will have a position related to the wavelength of the line and the star's location in the slit. If the PSF of the star is much larger than a slit width, then small shifts in the star's position should not result in a measurable shift in the

emission-line. The same considerations apply in the spatial direction along the slit. We have learned from Gemini that the intrinsic limit for a centroid measurement will be approximately 1/20 of a resolution element, so we can demand that the instrument be stable enough to maintain wavelength calibration to this level. This demand requires very precise alignment and stability of the image rotator as it rotates. Unfortunately, it is so difficult to achieve these goals, that we had to find other ways to satisfy them. We chose to require a telescope pointing model which would account for any error in boresighting the image rotator with respect to the input optical axis. This method will still achieve a net wandering of less than 1/20 of a resolution element at the slit plane, but it doesn't rely upon precise alignment to achieve it.

Spot size requirements and Lyot stop performance will dictate the degree to which the image rotator will collimate the beam and form a pupil image. We required less than 1% maximum offset of the pupil image at the Lyot stop due to pupil wander as the image rotator rotates. This amounts to 267 μm.

The image rotator design is shown in Figure 2. Rays for seven field points (corners of the SCAM FOV and the center and edges of the slit) are plotted. The trace starts at the Keck f/15 focus and ends at the Lyot stop/filter. The design utilizes three reflections to perform the image derotation, and an off-axis parabola (OAP) to provide the collimation and pupil image formation. The pupil image size is determined by the track length between the Keck focus and the OAP. As this distance becomes longer, the pupil image becomes larger.

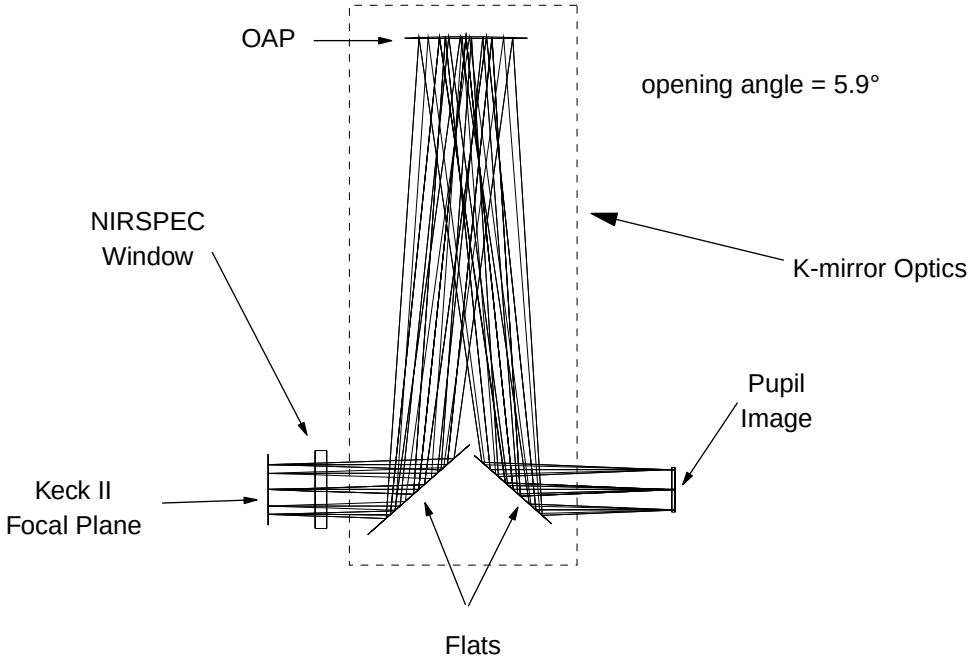

K-mirror Assembly and Surrounding Optics

Figure 2. Image rotator K-mirror design.

This form is aberration-free on-axis due to the imaging properties of a parabola. Figure 3 is a simple illustration showing that a parabola can be used in an unobstructed design where the central field point is still essentially an on-axis field point. This is the key to the aberration-free behavior of the design. The same principle is used in the f/converter and in the back-end design.

Principle of the Off-Axis Parabola (OAP)

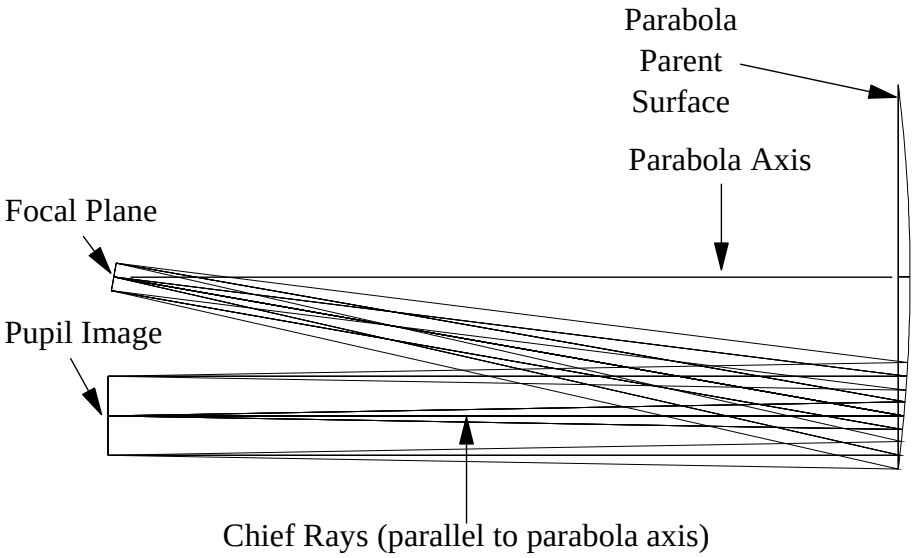

Figure 3

VII. F/converter Design

The f/converter takes the - 7° field and focusses the beams at the slit plane. In addition to forming an image of the object field, the f/converter will transfer an image of the pupil to the back end, thus defining the exit pupil of the front end. In order to minimize the size of the first element (collimator) of the back end, the f/converter should present an exit pupil which is nearly at infinity, i.e. the output beams will be telecentric. This would then allow the back end collimator to be placed at a distance equal to its focal length in order to form a pupil image at the echelle which would sit at a distance equal to the collimator focal length away from the collimator. Of course, small deviations from telecentricity will require that the echelle be placed at a distance which is slightly different than the focal length of the collimator; this is analogous to the situation of the Keck exit pupil, the IROT, and the Lyot stop. In that case, the Keck exit pupil is not quite at infinity, so the Lyot stop needs to be placed at a distance which is slightly larger than the focal length of the IROT.

Both refractive and reflective designs were considered for the f/converter. The best refractive doublet design is shown in Figure 4. Rays are traced from the Lyot stop/filter, through the lens, and onto the slit plane. This design was presented at the PDR, and it had very good performance except for extreme corners of the SCAM FOV. Of course, it also introduced chromatic aberrations which degraded the performance somewhat for extreme wavelengths.

A reflective design is shown in Figure 5. It has better performance than the refractive design due to the fact that it is inherently achromatic. Four forms were considered for the reflective design: 1). flat/sphere/flat, 2). cylinder/sphere/flat, 3). flat/toroid/flat, and 4). flat/OAP/flat. The second and third forms gave essentially the same performance because they are essentially the same forms with the only difference being the location of the non-axisymmetric power. The last form gave the best performance, and it became the final design.

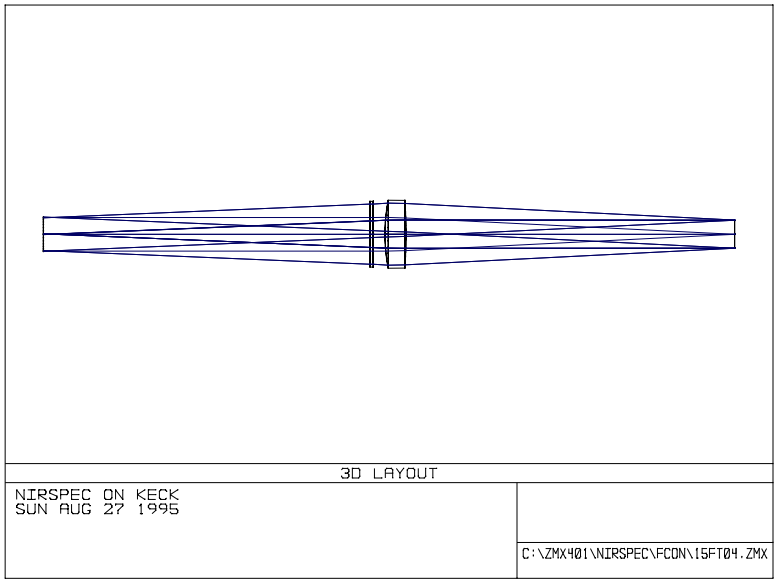

Figure 4. Refractive design with LiF/BaF_2 doublet.

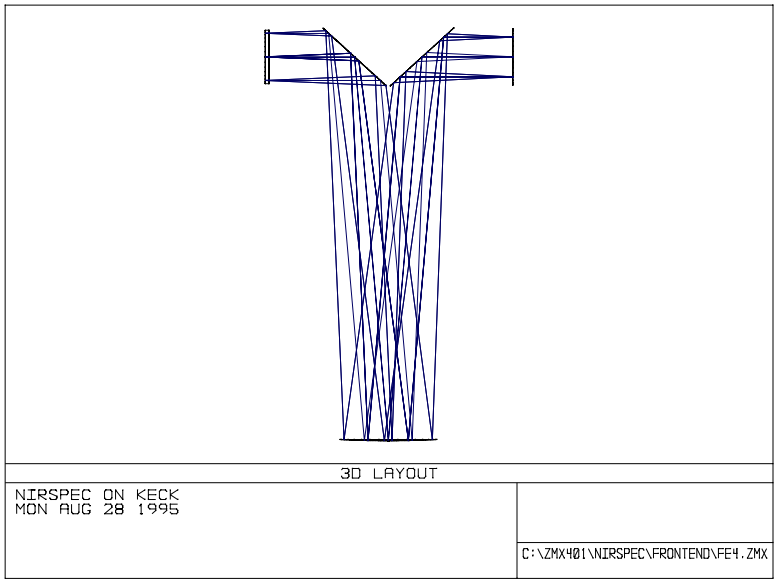

Figure 5. Reflective design.

VIII. Complete Front-end Design

A complete ray-trace for the front-end is shown in Figure 6. The IROT is shown in the nominal "zero degree" position, making its long axis parallel to the long axis of the f/converter K-mirror. This configuration counterbalances some of the aberrations introduced by the f/converter. Of course, this counterbalance is only best when the IROT is in the nominal position.

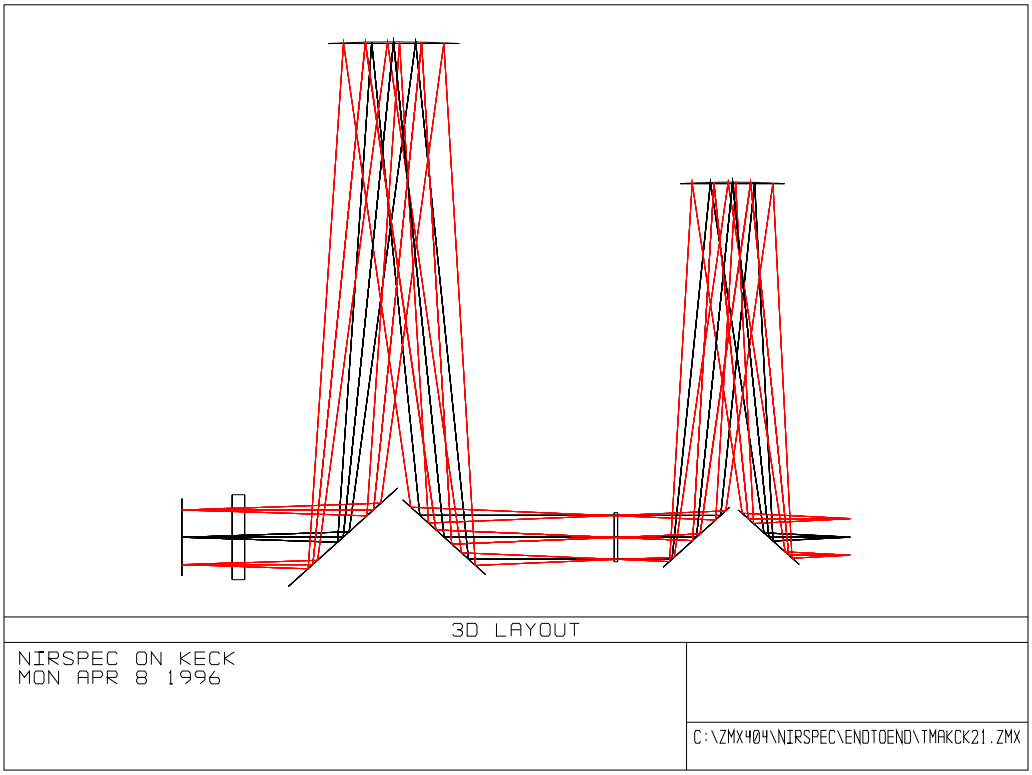

Figure 6. Ray trace for complete front-end.

The full optical prescription is given in Table 4. The distances and focal lengths in this prescription match the ideal numbers, discussed earlier, quite closely. I discuss some of these numbers below, where the surface numbers are shown in parentheses.

The distance between the secondary (3) and the telescope focal plane (4) is 17.89498 m. The apparent window thickness is its physical thickness multiplied by 1+(1-n)/n, where n is the index of the window material. In this case, the material is CaF_2, the index is -1.42 for λ - 2-3 μm, so the apparent thickness is 5.281690 mm. The apparent distance between the telescope focal plane and the IROT/collimator OAP surface (17) is 0.03063336 + 0.005281690 + 0.06 + 0.304085 = 0.400000 m. Note that this is the distance to the mirror surface where the chief ray of the axial field point intersects the parabola, not the distance to the parent vertex of the OAP. There is another 0.00408495 m (15) of distance in the model, along with a tilt in coordinate break 13, and an offset in coordinate break 14. These three items place the vertex of the OAP so that the OAP surface will intercept the beam after the beam has traveled an apparent distance of 0.4 m from the telescope focal plane. The

same tricks are used in leaving the OAP surface (see coordinate break 18). The distance from the IROT/collimator surface to the Lyot stop is 0.304085 + 0.1036465 = 0.408021 m.

The filter (24/25) has an apparent thickness of 0.001408 mm. Adding this to 0.048 m and 0.218002 m gives 0.267410 m for the apparent distance from the pupil image to the f/converter surface. Again, offsets (30 and 31) are used to place the OAP vertex in the proper position. The distance between the OAP and the slit plane has been set to 0.267424 m for best focus of the central field point. This is in contrast to the expected value of 0.267410 (= 26.7410 mm × 10). The difference is 14 μm, and I am not sure why this inconsistency exists. There is probably some cumulative offset which is generated by upstream elements. For instance, perhaps the telescope focal plane for the on-axis field point is not exactly at the distance I set between the secondary and surface 4. This would result in a slightly uncollimated beam between the IROT/collimator and the f/converter. This would result in a slight longitudinal shift of the front-end focus. In any case, 14 μm is less than manufacturing precision and alignment precision for the slit plane.

The on-axis focal length of the IROT/collimator OAP is 0.7918301 m. To the beam, however, this appears as 0.4 m. Likewise, the focal length of the OAP in the f/converter (32) appears to be 0.534820 m as seen by the input beam.

Table 4: Optical Surface Prescription for Front-end
all units in meters

System/Prescription Data

File : C:\ZMX404\NIRSPEC\FRONTEND\FE8.ZMX
Title: NIRSPEC ON KECK
Date : TUE APR 9 1996

SURFACE DATA SUMMARY:

Surf	Type	Radius	Thickness	Glass	Diameter	Conic
OBJ	STANDARD	Infinity	Infinity		0	0
1	STANDARD	Infinity	16.65		0.4914	0
STO	STANDARD	-34.974	-15.39499	MIRROR	10	-1.003683
3	STANDARD	-4.737916	17.89498	MIRROR	1.309857	-1.644326
4	STANDARD	Infinity	0.03063336		0.04718317	0
5	STANDARD	Infinity	0.0075	CAFL	0.04872591	0
6	STANDARD	Infinity	0.06		0.04899549	0
7	COORDBRK	--------	0		0	--------
8	COORDBRK	--------	0		0	--------
9	COORDBRK	--------	0		0	--------
10	STANDARD	Infinity	0	MIRROR	0.07043377	0
11	COORDBRK	--------	-0.304085		0	--------
12	COORDBRK	--------	0		0	--------
13	COORDBRK	--------	0		0	--------
14	COORDBRK	--------	0		0	--------
15	COORDBRK	--------	-0.00408495		0	--------
16	COORDBRK	--------	0		0	--------
17	STANDARD	0.7918301	0	MIRROR	0.2241023	-1
18	COORDBRK	--------	0.00408495		0	--------
19	COORDBRK	--------	0.304085		0	--------
20	COORDBRK	--------	0		0	--------
21	STANDARD	Infinity	0	MIRROR	0.0556804	0
22	COORDBRK	--------	-0.1036465		0	--------
23	COORDBRK	--------	0		0	--------
24	STANDARD	Infinity	-0.002	CAF2_77X	0.0274054	0
25	STANDARD	Infinity	-0.048		0.02728836	0
26	COORDBRK	--------	0		0	--------
27	COORDBRK	--------	0		0	--------
28	STANDARD	Infinity	0	MIRROR	0.04841444	0
29	COORDBRK	--------	0.2180015		0	--------
30	COORDBRK	--------	0		0	--------
31	COORDBRK	--------	0.00273089		0	--------
32	STANDARD	-0.5293582	0	MIRROR	0.158105	-1
33	COORDBRK	--------	-0.00273089		0	--------
34	COORDBRK	--------	0		0	--------
35	COORDBRK	--------	0		0	--------
36	COORDBRK	--------	-0.2180015		0	--------
37	COORDBRK	--------	0		0	--------
38	STANDARD	Infinity	0	MIRROR	0.04899811	0
39	COORDBRK	--------	0.04942265		0	--------
40	COORDBRK	--------	0		0	--------
41	COORDBRK	--------	0		0	--------
IMA	STANDARD	Infinity	0		0.03193434	0

IX. Front-end Performance

The performance is described in this section, mostly in the form of figures from Zemax. Figure 7 is a full figure spot diagram at the Lyot stop/filter. Figure 8 is a composite of spot diagrams at the slit focal plane for various field points and image rotator angles. Figure 9 is a table containing the RMS WFE for various field points and rotator angles. Figures 10, 11, 12, and 13 show the same thing in graphical form. Figure 14 shows the Strehl ratio versus field radius and wavelength.

The spot diagrams at the pupil show that the pupil image plane is tilted, so that rays at the top of the field have already passed through focus, and rays at the bottom of the field have not yet come to a focus. We could tilt the Lyot stop/filter assembly so that the assembly sits at the focus, but the tilted focal plane spins as the image rotator rotates, i.e. the whole pattern in Figure 7 spins around the optical axis. The largest spot cluster is 2% of the pupil image size.

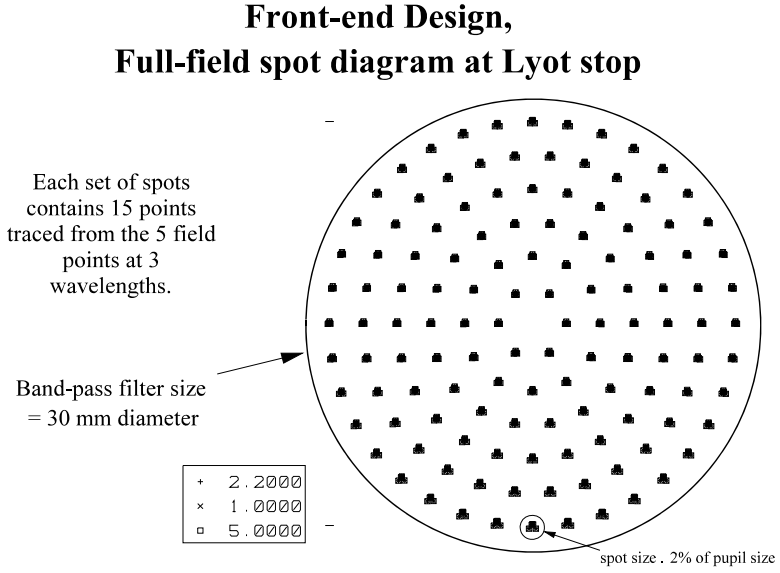

Figure 7

As seen in Figures 8 and 9, the on-axis performance is essentially perfect and well within the Rayleigh criterion for diffraction limited systems (WFE < $\lambda_{PV}/4$ - $\lambda_{RMS}/20$). In fact, the design satisfies this criterion for all field points within a 30″ slit and $\lambda > 2.75$ μm at $\theta_{IROT} = 0°$. This can be determined by scaling the values in Figure 9 in the following way: $WFE_{RMS,slit\ edge} = 0.125 \times (1.1$ μm / $\lambda) \times \lambda = 0.05 \times (2.75$ μm / $\lambda) \times \lambda < 0.05$ for $\lambda > 2.75$ μm. For $\lambda = 1$ μm, the Rayleigh criterion is satisfied for a 12″, or smaller, slit length. At the edge of the largest field (r = 23′ = 0.0064°), i.e. in the low-res or pure imaging modes, the system is strictly diffraction limited only for $\lambda \geq 4$ μm.

Figure 9 shows that the design quickly departs from being diffraction limited as the image rotator is moved out of the ideal position. For instance, the system is only diffraction-limited for $\lambda > 5.5$ μm at the edge of the 30″ slit and $\theta_{IROT} = 45°$.

We can draw a straight line through the curves in Figures 10, 11, 12, and 13 to determine a linear relationship between WFE, λ, and field position. As an example, consider the curve for 1 μm in Figure 10. We can fit the line so that it goes through the point at 0.005° (r = 180), where the WFE is - 0.18 Å 1 μm. Using this fit, the RMS WFE will be given by equation 2. This equation is in rough agreement with the numbers in Figure 9. For instance, the equation would indicate that the system is diffraction-limited for $\lambda > 3$ μm and r < 150, while, as we saw above, Figure 9 gives $\lambda >$ 2.75 μm for r < 150.

$$WFE_{RMS} = \left(\frac{0.18\,\mu m}{\lambda}\right)\left(\frac{r''}{18''}\right)\lambda = 0.01\left(\frac{r''}{\lambda}\right)\lambda < 0.05\lambda, \text{ for } \frac{r''}{\lambda} < 5.0. \qquad (2)$$

We can find similar relations for each image rotator position. The only change is in the scaling coefficient (0.01). Repeating the exercise above, we get the following limits in r0/λ for diffraction-limited performance: 4.0 (θ_{IROT} = 22.5°), 2.6 (θ_{IROT} = 45°), and 1.6 (θ_{IROT} = 90°).

More important than whether the system is diffraction limited is whether it meets the performance specification, i.e. 80% ensquared energy (ESE) within 1 spectrometer pixel. This can be determined from Figure 9 where 3 cases for θ_{IROT} are shown. It is seen that the performance criterion is met for all θ_{IROT}, all slit field points (in the high-res mode), and one of the shortest wavelengths to pass through the system. Values for the "slit edges" refer to a 30 slit. In the real system, the slit length in the high-res mode will be limited to less than half of this value for $\lambda < 2$ μm. For longer wavelengths, the ESE will be dominated by diffraction, and the ESE will be > 80% everywhere in the slit.

Front-end Design, Spots for Various θ_{IROT}

Box size is 97 μm = 0.″2 = 1/2 slit width = 1.4 pixel widths

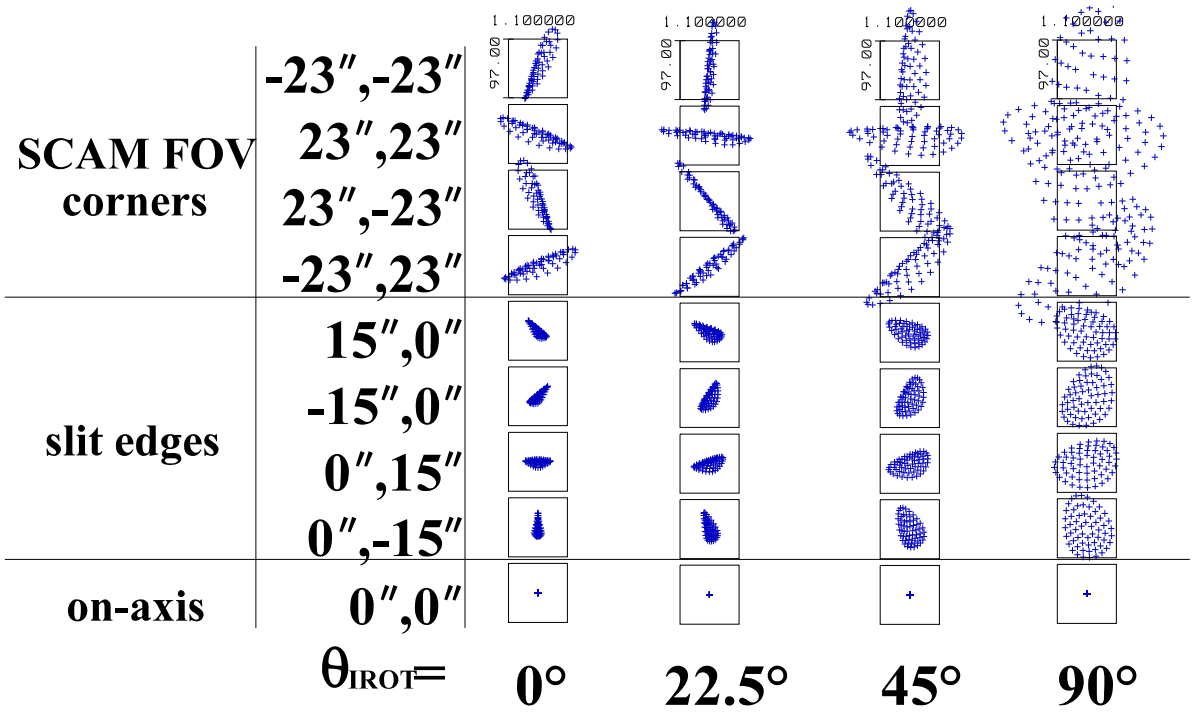

Figure 8

Front-end Design, Performance Numbers

Evaluated at slit plane, λ=1.1 μm, ensquared energy (ESE) includes diffraction

1/2 slit width = 0.″2, 1 spectrometer pixel = 0.″145, SCAM pixel = 0.″18

θ_{IROT}= 0°

	RMS Spot Size μm	RMS WFE $\lambda_{1.1\,\mu m}$	ESE in 1/2 Slit %	ESE in 1 spec. pixel %	ESE in SCAM pixel %
central f.p.	0	0.000	96	95	95
slit edges	11	0.125	96	95	95
SCAM corners	34	0.330	90	NA	87

θ_{IROT}=45°

	RMS Spot Size μm	RMS WFE $\lambda_{1.1\,\mu m}$	ESE in 1/2 Slit %	ESE in 1 spec. pixel %	ESE in SCAM pixel %
central f.p.	0	0.000	96	95	95
slit edges	21	0.250	96	91	93
SCAM corners	51	0.575	70	NA	62

θ_{IROT}=90°

	RMS Spot Size μm	RMS WFE $\lambda_{1.1\,\mu m}$	ESE in 1/2 Slit %	ESE in 1 spec. pixel %	ESE in SCAM pixel %
central f.p.	0	0.000	96	95	95
slit edges	34	0.420	90	82	88
SCAM corners	79	0.930	37	NA	34

Figure 9

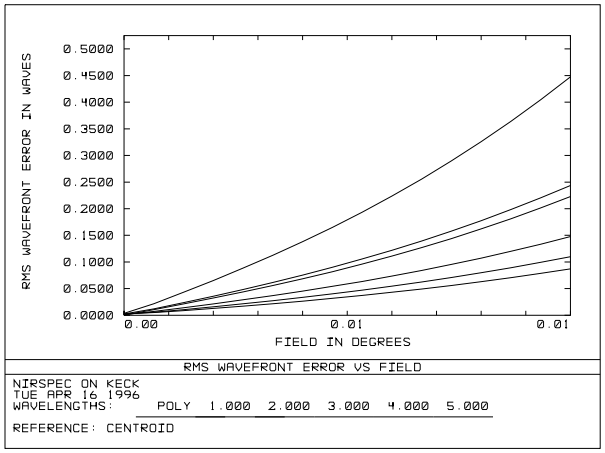

Figure 10. RMS WFE versus wavelength and field position for θ_{IROT} = 0°. Curves are for 1 μm, polychromatic, 2 μm, 3 μm, 4 μm, and 5 μm from top to bottom. Diffraction-limited corresponds to 0.05 RMS WFE. A 30″ long slit corresponds to a radius of 0.0042°. The SCAM FOV edge corresponds to a radius of 0.0064°. The SCAM FOV corners corresponds to a radius of 0.0090°. The x-axis extends to 0.0100°.

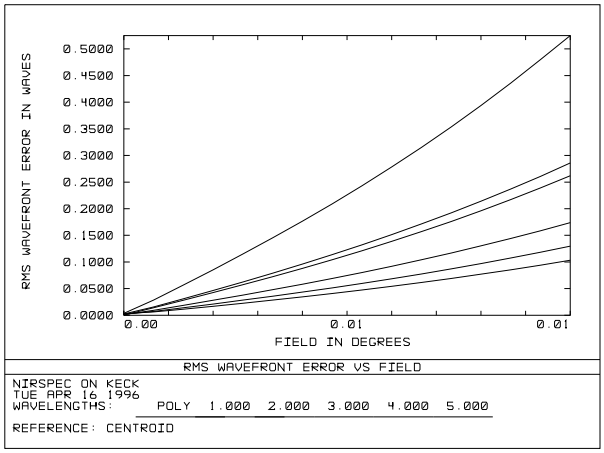

Figure 11. Same as for Figure 10, and θ_{IROT}= 22.5°.

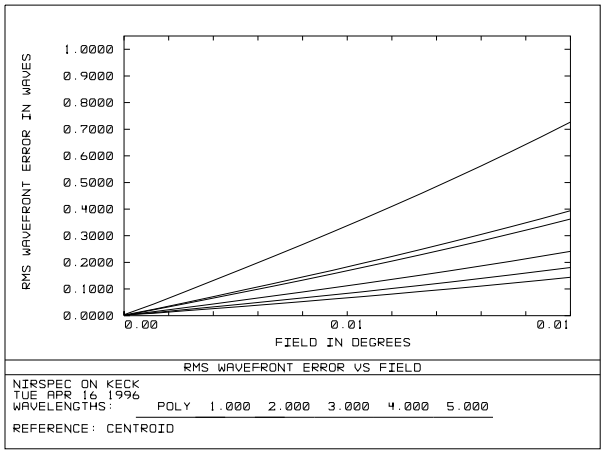

Figure 12 . Same as for Figure 10, and θ_{IROT} = 45°. Vertical axis scale is twice that in Figure 10.

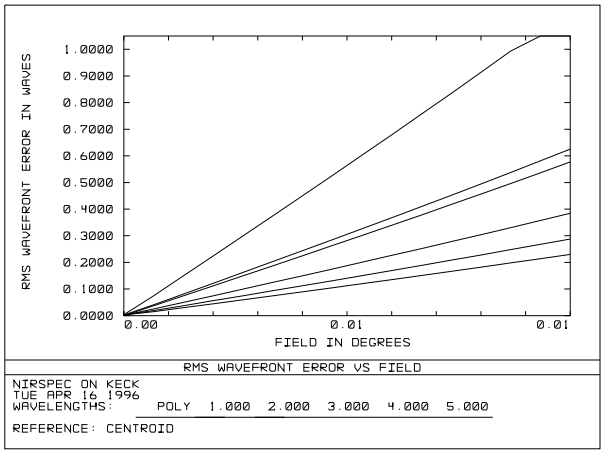

Figure 13. Same as for Figure 10, and θ_{IROT} = 90°. Vertical axis scale is twice that in Figure 10.

Front-end Design, Strehl Ratio
θ_{IROT}=0°

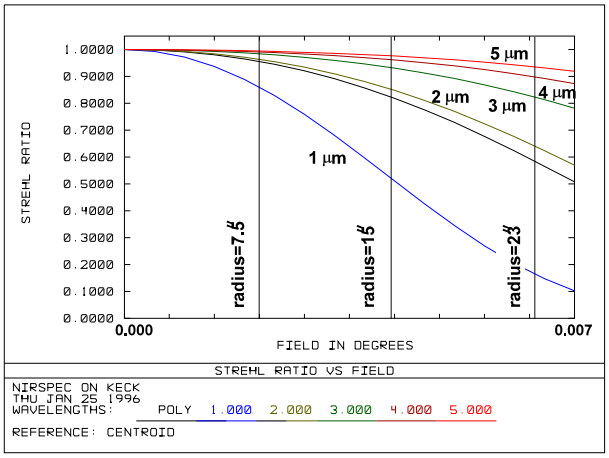

Figure 14. Strehl ratio versus field radius and wavelength for θ_{IROT} = 0°. The unlabeled curve represents a polychromatic average over all wavelengths. A diffraction-limited system (Rayleigh criterion) will have a Strehl ratio of 0.80 if the aberrations are mostly defocus (see p. 337 in Smith's book). This criterion would indicate that the system is diffraction-limited for $r0/\lambda < 8$, a much less stringent value than in equation 2. This difference is due to the fact that the front-end aberrations are not simply due to defocus.

Appendix A: Full Optical Prescription for Front-end

```
System/Prescription Data

File : C:\ZMX404\NIRSPEC\FRONTEND\FE8.ZMX
Title: NIRSPEC ON KECK
Date : TUE APR 9 1996

GENERAL LENS DATA:

Surfaces        :          42
Stop            :           2
System Aperture :Entrance Pupil Diameter
Ray aiming      : Off
Apodization     :Uniform, factor =     0.000000
Eff. Focal Len. :    -100.111 (in air)
Eff. Focal Len. :    -100.111 (in image space)
Total Track     :     19.3152
Image Space F/# :     10.0111
Working F/#     :     10.0035
Obj. Space N.A. :      5e-010
Stop Radius     :           5
Parax. Ima. Hgt.:    0.015787
Parax. Mag.     :           0
Entr. Pup. Dia. :          10
Entr. Pup. Pos. :       16.65
Exit Pupil Dia. :    0.518579
Exit Pupil Pos. :     5.18243
Field Type      : Angle in degrees
Maximum Field   :  0.00903527
Primary Wave    :    2.200000
Lens Units      :      Meters
Angular Mag.    :     19.2835

Fields          : 9
Field Type: Angle in degrees
#         X-Value         Y-Value          Weight
1       -0.006389       -0.006389        0.000000
2        0.006389        0.006389        0.000000
3        0.006389       -0.006389        0.000000
4       -0.006389        0.006389        0.000000
5        0.004167        0.000000        0.000000
6       -0.004167        0.000000        0.000000
7        0.000000        0.004167        0.000000
8        0.000000       -0.004167        0.000000
9        0.000000        0.000000        1.000000

Vignetting Factors
#        VDX       VDY       VCX       VCY
1  0.000000  0.000000  0.000000  0.000000
2  0.000000  0.000000  0.000000  0.000000
3  0.000000  0.000000  0.000000  0.000000
4  0.000000  0.000000  0.000000  0.000000
5  0.000000  0.000000  0.000000  0.000000
6  0.000000  0.000000  0.000000  0.000000
7  0.000000  0.000000  0.000000  0.000000
8  0.000000  0.000000  0.000000  0.000000
9  0.000000  0.000000  0.000000  0.000000

Wavelengths     : 1
Units: Microns
#           Value          Weight
1       2.200000        1.000000

SURFACE DATA SUMMARY:

Surf     Type       Radius    Thickness        Glass     Diameter       Conic
 OBJ STANDARD     Infinity     Infinity                         0           0
   1 STANDARD     Infinity        16.65                    0.4914           0
 STO STANDARD      -34.974    -15.39499       MIRROR           10   -1.003683
   3 STANDARD    -4.737916     17.89498       MIRROR     1.309857   -1.644326
   4 STANDARD     Infinity   0.03063336                0.04718317           0
   5 STANDARD     Infinity       0.0075         CAFL   0.04872591           0
   6 STANDARD     Infinity         0.06                0.04899549           0
   7 COORDBRK     --------            0                         0     --------
   8 COORDBRK     --------            0                         0     --------
   9 COORDBRK     --------            0                         0     --------
  10 STANDARD     Infinity            0       MIRROR   0.07043377           0
  11 COORDBRK     --------    -0.304085                         0     --------
  12 COORDBRK     --------            0                         0     --------
  13 COORDBRK     --------            0                         0     --------
  14 COORDBRK     --------            0                         0     --------
  15 COORDBRK     --------  -0.00408495                         0     --------
  16 COORDBRK     --------            0                         0     --------
```

17	STANDARD	0.7918301	0	MIRROR	0.2241023	-1
18	COORDBRK	--------	0.00408495		0	--------
19	COORDBRK	--------	0.304085		0	--------
20	COORDBRK	--------	0		0	--------
21	STANDARD	Infinity	0	MIRROR	0.0556804	0
22	COORDBRK	--------	-0.1036465		0	--------
23	COORDBRK	--------	0		0	--------
24	STANDARD	Infinity	-0.002	CAF2_77X	0.0274054	0
25	STANDARD	Infinity	-0.048		0.02728836	0
26	COORDBRK	--------	0		0	--------
27	COORDBRK	--------	0		0	--------
28	STANDARD	Infinity	0	MIRROR	0.04841444	0
29	COORDBRK	--------	0.2180015		0	--------
30	COORDBRK	--------	0		0	--------
31	COORDBRK	--------	0.00273089		0	--------
32	STANDARD	-0.5293582	0	MIRROR	0.158105	-1
33	COORDBRK	--------	-0.00273089		0	--------
34	COORDBRK	--------	0		0	--------
35	COORDBRK	--------	0		0	--------
36	COORDBRK	--------	-0.2180015		0	--------
37	COORDBRK	--------	0		0	--------
38	STANDARD	Infinity	0	MIRROR	0.04899811	0
39	COORDBRK	--------	0.04942265		0	--------
40	COORDBRK	--------	0		0	--------
41	COORDBRK	--------	0		0	--------
IMA	STANDARD	Infinity	0		0.03193434	0

SURFACE DATA DETAIL:

Surface OBJ : STANDARD
Surface 1 : STANDARD
Aperture : Circular
Obscuration
Minimum Radius : 0
Maximum Radius : 0.6549285
Surface STO : STANDARD
Aperture : Circular
Aperture
Minimum Radius : 0.6549285
Maximum Radius : 1e+010
Surface 3 : STANDARD
Surface 4 : STANDARD
Surface 5 : STANDARD
Aperture : Circular
Aperture
Minimum Radius : 0
Maximum Radius : 0.026
Surface 6 : STANDARD
Aperture : Circular
Aperture
Minimum Radius : 0
Maximum Radius : 0.026
Surface 7 : COORDBRK
Decenter X : 0
Decenter Y : 0
Tilt About X : 0
Tilt About Y : 0
Tilt About Z : 180
Surface 8 : COORDBRK
Decenter X : 0
Decenter Y : 0
Tilt About X : 0
Tilt About Y : 0
Tilt About Z : 0
Surface 9 : COORDBRK
Decenter X : 0
Decenter Y : 0
Tilt About X : -47.9
Tilt About Y : 0
Tilt About Z : 0
Surface 10 : STANDARD
Aperture : Rectangular
Aperture
X Half Width : 0.02905
Y Half Width : 0.0448
Surface 11 : COORDBRK
Decenter X : 0
Decenter Y : 0
Tilt About X : -47.9
Tilt About Y : 0
Tilt About Z : 0
Surface 12 : COORDBRK
Decenter X : 0
Decenter Y : 0
Tilt About X : 0
Tilt About Y : 0
Tilt About Z : 0
Surface 13 : COORDBRK
Decenter X : 0
Decenter Y : 0
Tilt About X : 11.6
Tilt About Y : 0
Tilt About Z : 0
Surface 14 : COORDBRK
Decenter X : 0
Decenter Y : 0.08043117
Tilt About X : 0
Tilt About Y : 0
Tilt About Z : 0
Surface 15 : COORDBRK
Decenter X : 0
Decenter Y : 0
Tilt About X : 0
Tilt About Y : 0
Tilt About Z : 0
Surface 16 : COORDBRK
Decenter X : 0
Decenter Y : 0
Tilt About X : 0
Tilt About Y : 0
Tilt About Z : 0
Surface 17 : STANDARD
Aperture : Circular
Aperture
Minimum Radius : 0
Maximum Radius : 0.0396
Y- Decenter : -0.0804312
Surface 18 : COORDBRK
Decenter X : 0
Decenter Y : -0.08043117
Tilt About X : 0
Tilt About Y : 0
Tilt About Z : 0
Surface 19 : COORDBRK
Decenter X : 0
Decenter Y : 0
Tilt About X : 0
Tilt About Y : 0
Tilt About Z : 0
Surface 20 : COORDBRK
Decenter X : 0
Decenter Y : 0
Tilt About X : -47.9
Tilt About Y : 0
Tilt About Z : 0
Surface 21 : STANDARD
Aperture : Rectangular
Aperture
X Half Width : 0.02015
Y Half Width : 0.034
Surface 22 : COORDBRK
Decenter X : 0
Decenter Y : 0
Tilt About X : -47.9
Tilt About Y : 0
Tilt About Z : 0
Surface 23 : COORDBRK
Decenter X : 0
Decenter Y : 0
Tilt About X : 0
Tilt About Y : 0
Tilt About Z : 0
Surface 24 : STANDARD
Aperture : Circular
Aperture
Minimum Radius : 0
Maximum Radius : 0.015
Surface 25 : STANDARD
Aperture : Circular
Aperture
Minimum Radius : 0
Maximum Radius : 0.015
Surface 26 : COORDBRK
Decenter X : 0
Decenter Y : 0
Tilt About X : 0
Tilt About Y : 0
Tilt About Z : 0
Surface 27 : COORDBRK
Decenter X : 0
Decenter Y : 0
Tilt About X : -47.9
Tilt About Y : 0
Tilt About Z : 0
Surface 28 : STANDARD
Aperture : Rectangular
Aperture
X Half Width : 0.01745
Y Half Width : 0.02732
Surface 29 : COORDBRK
Decenter X : 0
Decenter Y : 0
Tilt About X : -47.9
Tilt About Y : 0
Tilt About Z : 0
Surface 30 : COORDBRK
Decenter X : 0
Decenter Y : 0.05377025
Tilt About X : 0
Tilt About Y : 0
Tilt About Z : 0
Surface 31 : COORDBRK
Decenter X : 0
Decenter Y : 0
Tilt About X : 0
Tilt About Y : 0
Tilt About Z : 0
Surface 32 : STANDARD
Aperture : Circular
Aperture
Minimum Radius : 0
Maximum Radius : 0.03153
Y- Decenter : -0.0537703
Surface 33 : COORDBRK

```
 Decenter X     :             0
 Decenter Y     :             0
 Tilt About X   :             0
 Tilt About Y   :             0
 Tilt About Z   :             0
Surface  34     : COORDBRK
 Decenter X     :             0
 Decenter Y     :   -0.05377025
 Tilt About X   :             0
 Tilt About Y   :             0
 Tilt About Z   :             0
Surface  35     : COORDBRK
 Decenter X     :             0
 Decenter Y     :             0
 Tilt About X   :          11.6
 Tilt About Y   :             0
 Tilt About Z   :             0
Surface  36     : COORDBRK
 Decenter X     :             0
 Decenter Y     :             0
 Tilt About X   :             0
 Tilt About Y   :             0
 Tilt About Z   :             0
Surface  37     : COORDBRK
 Decenter X     :             0
 Decenter Y     :             0
 Tilt About X   :         -47.9
 Tilt About Y   :             0
 Tilt About Z   :             0
Surface  38     : STANDARD
  Aperture          : Rectangular
Aperture
 X Half Width   :       0.03145
 Y Half Width   :        0.0248
  X- Decenter   :         0.01515
Surface  39     : COORDBRK
 Decenter X     :             0
 Decenter Y     :             0
 Tilt About X   :         -47.9
 Tilt About Y   :             0
 Tilt About Z   :             0
Surface  40     : COORDBRK
 Decenter X     :             0
 Decenter Y     :             0
 Tilt About X   :             0
 Tilt About Y   :             0
 Tilt About Z   :             0
Surface  41     : COORDBRK
 Decenter X     :             0
 Decenter Y     :             0
 Tilt About X   :             0
 Tilt About Y   :             0
 Tilt About Z   :           180
Surface IMA     : STANDARD
  Aperture          : Rectangular
Aperture
 X Half Width   :        0.0115
 Y Half Width   :        0.0115


MULTI-CONFIGURATION DATA:

 Configuration   1:
 Param 5     8 :             0
 X-field     8 :             0
 Y-field     8 :  -0.004166666
 X-field     1 :    -0.0063889
 Y-field     1 :    -0.0063889
 X-field     2 :     0.0063889
 Y-field     2 :     0.0063889
 X-field     3 :     0.0063889
 Y-field     3 :    -0.0063889
 X-field     4 :    -0.0063889
 Y-field     4 :     0.0063889
 X-field     5 :   0.004166666
 Y-field     5 :             0
 X-field     6 :  -0.004166666
 Y-field     6 :             0
 X-field     7 :             0
 Y-field     7 :   0.004166666

 Configuration   2:
 Param 5     8 :          22.5
 X-field     8 :    0.00294628
 Y-field     8 :   -0.00294628
```

```
 X-field     1 :             0
 Y-field     1 :   -0.00903524
 X-field     2 :             0
 Y-field     2 :    0.00903524
 X-field     3 :    0.00903524
 Y-field     3 :             0
 X-field     4 :   -0.00903524
 Y-field     4 :             0
 X-field     5 :    0.00294628
 Y-field     5 :    0.00294628
 X-field     6 :   -0.00294628
 Y-field     6 :   -0.00294628
 X-field     7 :   -0.00294628
 Y-field     7 :    0.00294628

 Configuration   3:
 Param 5     8 :            45
 X-field     8 :   0.004166667
 Y-field     8 :             0
 X-field     1 :   0.006388889
 Y-field     1 :  -0.006388889
 X-field     2 :  -0.006388889
 Y-field     2 :   0.006388889
 X-field     3 :   0.006388889
 Y-field     3 :   0.006388889
 X-field     4 :  -0.006388889
 Y-field     4 :  -0.006388889
 X-field     5 :             0
 Y-field     5 :   0.004166667
 X-field     6 :             0
 Y-field     6 :  -0.004166667
 X-field     7 :  -0.004166667
 Y-field     7 :             0

 Configuration   4:
 Param 5     8 :            90
 X-field     8 :             0
 Y-field     8 :   0.004166666
 X-field     1 :   0.006388888
 Y-field     1 :   0.006388889
 X-field     2 :  -0.006388889
 Y-field     2 :  -0.006388889
 X-field     3 :    -0.0063889
 Y-field     3 :   0.006388889
 X-field     4 :   0.006388889
 Y-field     4 :  -0.006388889
 X-field     5 :  -0.004166667
 Y-field     5 :             0
 X-field     6 :   0.004166667
 Y-field     6 :             0
 X-field     7 :             0
 Y-field     7 :  -0.004166667

SOLVE AND VARIABLE DATA:

Semi Diam   1      : Fixed
Semi Diam   2      : Fixed
Semi Diam   3      : Fixed
Parameter  5 Surf  23: Pickup from 8 times 1.000000
Thickness of  33   : Solve, pick up value from 31, scaled by -1.00000
Thickness of  36   : Solve, pick up value from 29, scaled by -1.00000
Parameter  5 Surf  41: Pickup from 7 times 1.000000

INDEX OF REFRACTION DATA:

Surf     Glass      2.200000
   0              1.00000000
   1              1.00000000
   2    MIRROR    1.00000000
   3    MIRROR    1.00000000
   4              1.00000000
   5      CAFL    1.42280773
   6              1.00000000
   7              1.00000000
   8              1.00000000
   9              1.00000000
  10    MIRROR    1.00000000
  11              1.00000000
  12              1.00000000
  13              1.00000000
  14              1.00000000
  15              1.00000000
  16              1.00000000
  17    MIRROR    1.00000000
  18              1.00000000
  19              1.00000000
```

20		1.00000000
21	MIRROR	1.00000000
22		1.00000000
23		1.00000000
24	CAF2_77X	1.42499297
25		1.00000000
26		1.00000000
27		1.00000000
28	MIRROR	1.00000000
29		1.00000000
30		1.00000000
31		1.00000000
32	MIRROR	1.00000000
33		1.00000000
34		1.00000000
35		1.00000000
36		1.00000000
37		1.00000000
38	MIRROR	1.00000000
39		1.00000000
40		1.00000000
41		1.00000000
42		1.00000000

F/# DATA:

Wavelength: 2.200000

#	Field	Tan	Sag
1	-0.0064, -0.0064 deg:	10.1753	10.0029
2	0.0064, 0.0064 deg:	9.8340	10.0029
3	0.0064, -0.0064 deg:	10.1753	10.0029
4	-0.0064, 0.0064 deg:	9.8340	10.0029
5	0.0042, 0.0000 deg:	10.0031	10.0033
6	-0.0042, 0.0000 deg:	10.0031	10.0033
7	0.0000, 0.0042 deg:	9.8930	10.0035
8	0.0000, -0.0042 deg:	10.1156	10.0034
9	0.0000, 0.0000 deg:	10.0035	10.0035

GLOBAL VERTEX COORDINATES AND DIRECTIONS:

Surf	X coord	Y coord	Z coord	X direc	Y direc	Z direc
1	0.000000	0.000000	0.000000	0.000000	0.000000	1.000000
2	0.000000	0.000000	16.650000	0.000000	0.000000	1.000000
3	0.000000	0.000000	1.255015	0.000000	0.000000	1.000000
4	0.000000	0.000000	19.150000	0.000000	0.000000	1.000000
5	0.000000	0.000000	19.180633	0.000000	0.000000	1.000000
6	0.000000	0.000000	19.188133	0.000000	0.000000	1.000000
7	0.000000	0.000000	19.248133	0.000000	0.000000	1.000000
8	0.000000	0.000000	19.248133	0.000000	0.000000	1.000000
9	0.000000	0.000000	19.248133	0.000000	-0.741976	0.670427
10	0.000000	0.000000	19.248133	0.000000	-0.741976	0.670427
11	0.000000	0.000000	19.248133	0.000000	-0.994881	-0.101056
12	-0.000000	0.302528	19.278863	0.000000	-0.994881	-0.101056
13	-0.000000	0.302528	19.278863	0.000000	-0.994881	0.101056
14	-0.000000	0.294400	19.198844	0.000000	-0.994881	0.101056
15	-0.000000	0.294400	19.198844	0.000000	-0.994881	0.101056
16	-0.000000	0.298464	19.198431	0.000000	-0.994881	0.101056
17	-0.000000	0.298464	19.198431	0.000000	-0.994881	0.101056
18	-0.000000	0.306592	19.278450	0.000000	-0.994881	0.101056
19	-0.000000	0.302528	19.278863	0.000000	-0.994881	0.101056
20	0.000000	-0.000000	19.309593	0.000000	-0.741976	-0.670427
21	0.000000	-0.000000	19.309593	0.000000	-0.741976	-0.670427
22	0.000000	-0.000000	19.309593	-0.000000	0.000000	-1.000000
23	0.000000	-0.000000	19.413239	-0.000000	0.000000	-1.000000
24	0.000000	-0.000000	19.413239	-0.000000	0.000000	-1.000000
25	0.000000	-0.000000	19.415239	-0.000000	0.000000	-1.000000
26	0.000000	-0.000000	19.463239	-0.000000	0.000000	-1.000000
27	0.000000	-0.000000	19.463239	-0.000000	0.741976	-0.670427
28	0.000000	-0.000000	19.463239	-0.000000	0.741976	-0.670427
29	0.000000	-0.000000	19.463239	-0.000000	0.994881	0.101056
30	-0.000000	0.211452	19.538765	-0.000000	0.994881	0.101056
31	-0.000000	0.211452	19.538765	-0.000000	0.994881	0.101056
32	-0.000000	0.214169	19.539041	-0.000000	0.994881	0.101056
33	-0.000000	0.214169	19.539041	-0.000000	0.994881	0.101056
34	-0.000000	0.216886	19.485270	-0.000000	0.994881	0.101056
35	-0.000000	0.216886	19.485270	-0.000000	0.994881	-0.101056
36	-0.000000	0.216886	19.485270	-0.000000	0.994881	-0.101056
37	0.000000	-0.000000	19.507300	-0.000000	0.741976	0.670427
38	0.000000	-0.000000	19.507300	-0.000000	0.741976	0.670427
39	0.000000	-0.000000	19.507300	0.000000	-0.000000	1.000000
40	0.000000	-0.000000	19.556723	0.000000	-0.000000	1.000000
41	0.000000	-0.000000	19.556723	0.000000	-0.000000	1.000000
42	0.000000	-0.000000	19.556723	0.000000	-0.000000	1.000000

ELEMENT VOLUME DATA:

Units are cubic cm.

```
Values are only accurate for plane and spherical surfaces.
Element surf   5 to   6 volume :      14.062759
Element surf  24 to  25 volume :       1.174723
```

Appendix B: Aperture Sizes

4.3 Qualified Clear Apertures

Clear aperture diagrams are shown in the following 6 figures. The rotator angle refers to the angular position of the image rotator assembly about the input optical axis. In some cases, we overlaid two separate sets of spots for rotator angle = 0° and 45° in order to generate the full aperture size. The final dimensions were calculated to give 2 mm of extra space around the beam footprint for each part. Because this extra space is defined in terms of the beam, we require about 3 mm of extra surface on diagonally tilted flats.

Figure 20 shows the special case for the last flat in the FCON k-mirror. The beams reflect off this flat (black dots) onto the slit plane mirror surface, then reflect back onto the flat (grey dots). The size is longer in the x-axis, and the aperture is offset by 15.15 mm.

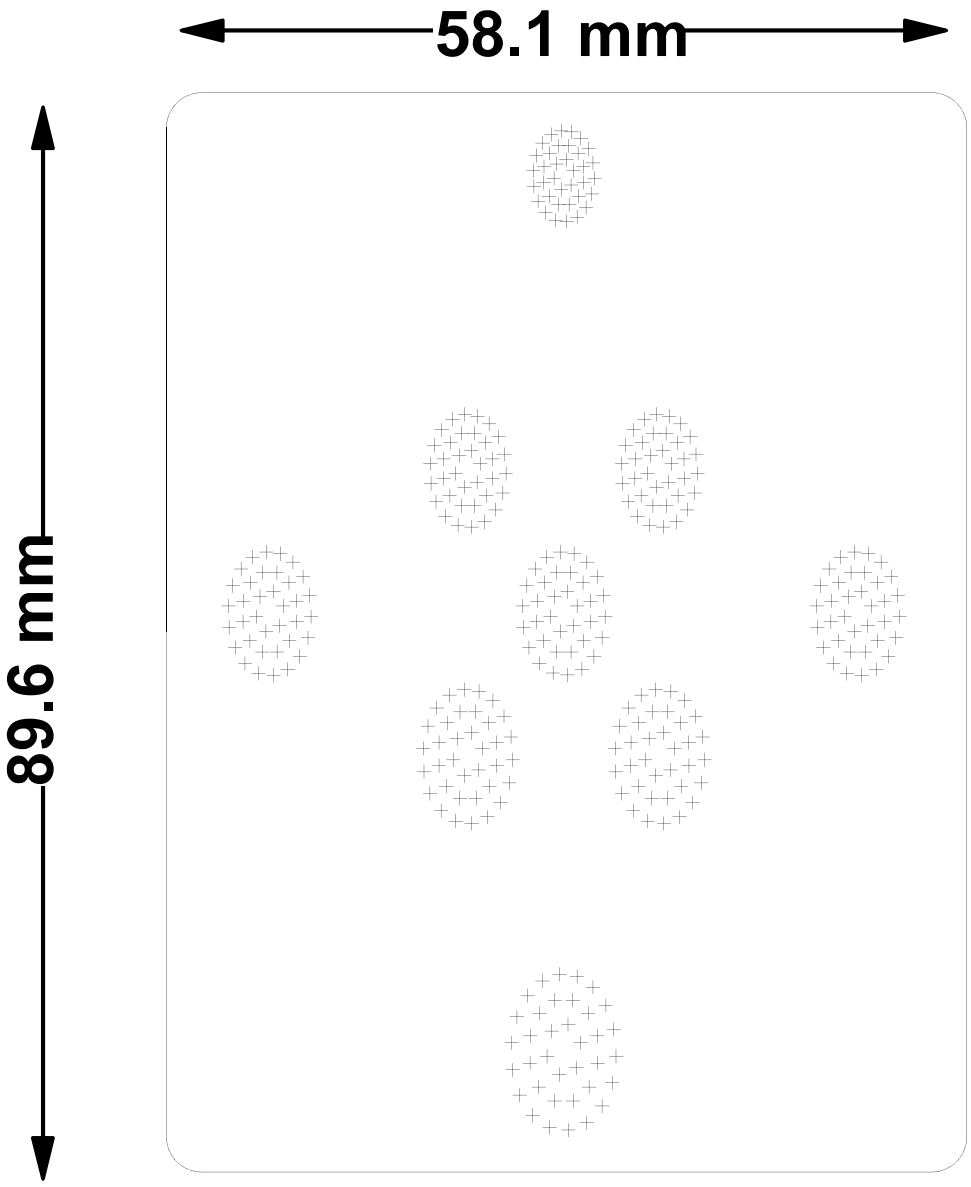

F 1

Rotator angle = 45

Figure 15

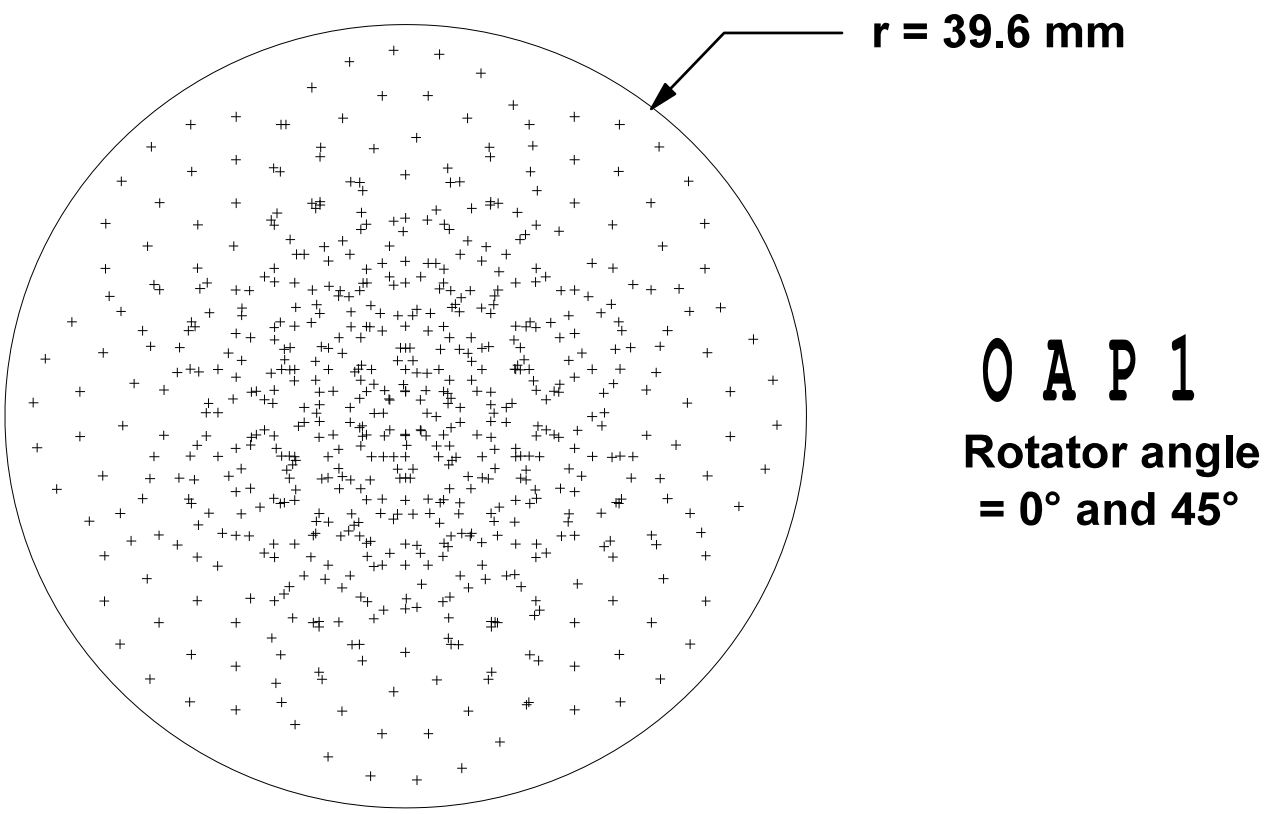

Figure 16

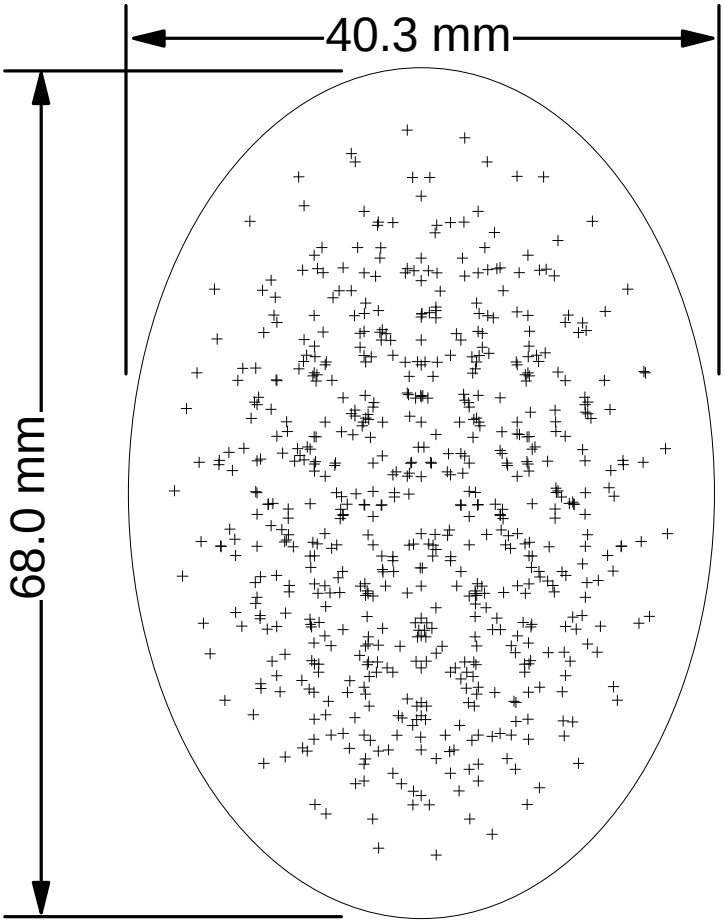

F2

Rotator angle
= 0° and 45°

Figure 17

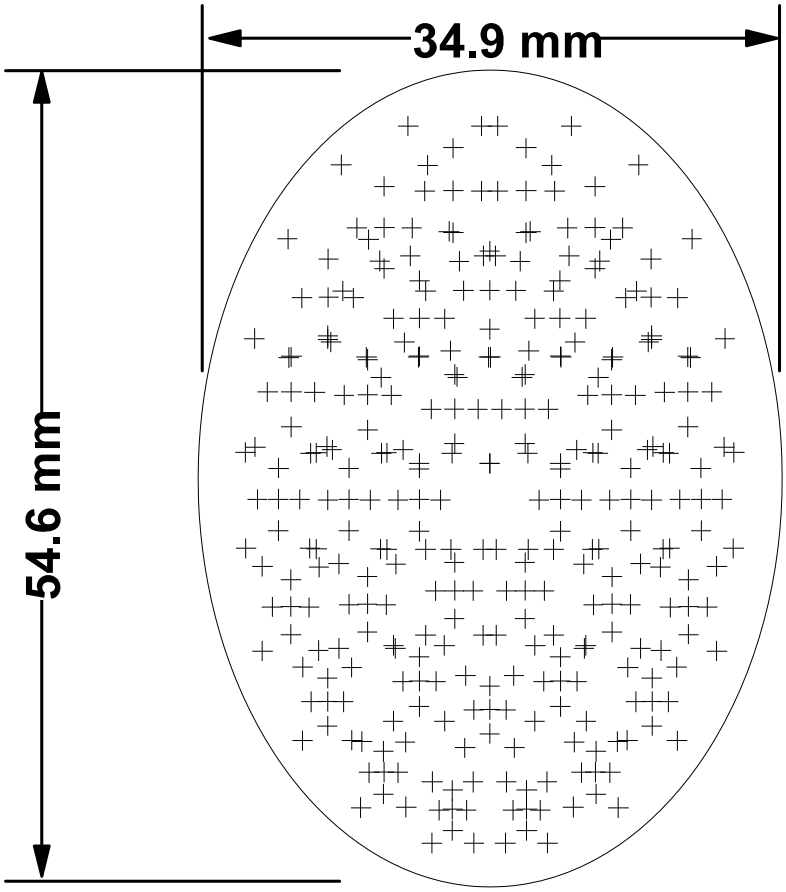

F 3

Figure 18

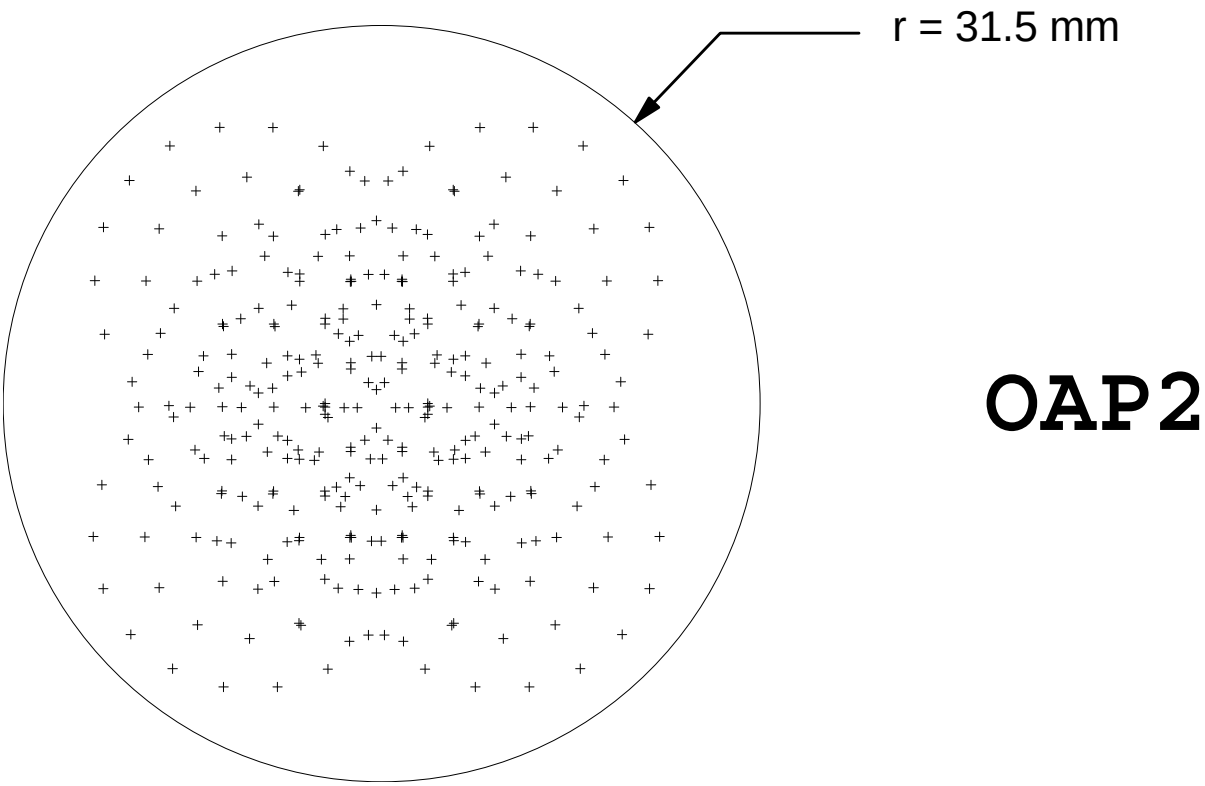

Figure 19

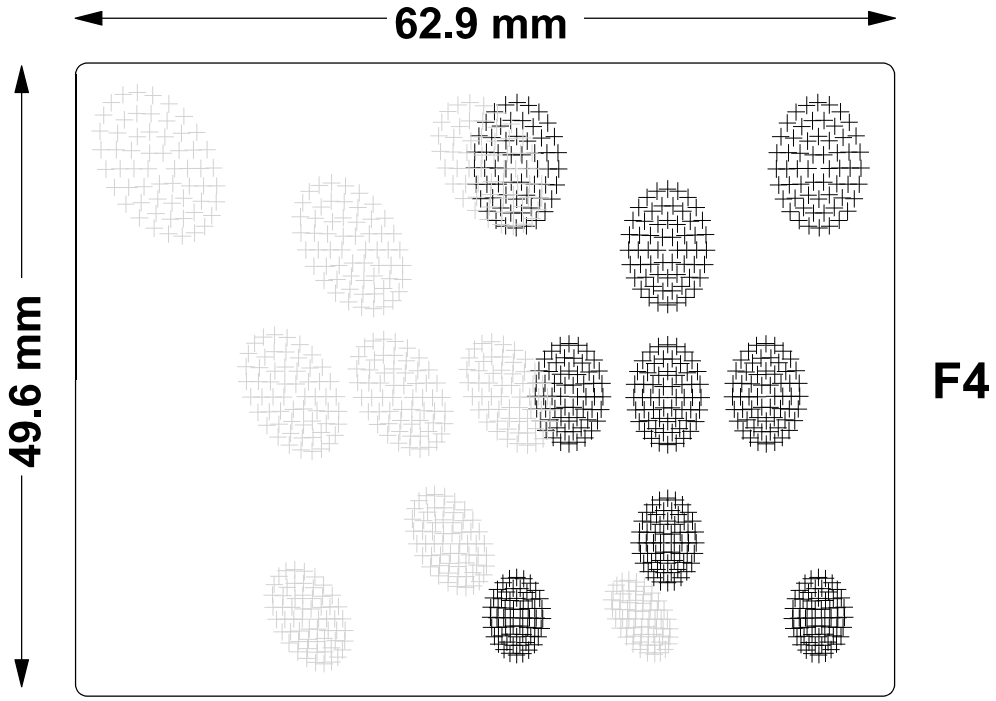

Figure 20